Pulmonary Inflammation After Intraperitoneal Administration of Ultrafine Titanium Dioxide (TiO$_2$) At Rest or in Lungs Primed with Lipopolysaccharide

Changsuk Moon , Hyun-Jeong Park , Youn-Hee Choi , Eun-Mi Park , Vincent Castranova & Jihee Lee Kang

Taylor & Francis
Taylor & Francis Group

PULMONARY INFLAMMATION AFTER INTRAPERITONEAL ADMINISTRATION OF ULTRAFINE TITANIUM DIOXIDE (TiO$_2$) AT REST OR IN LUNGS PRIMED WITH LIPOPOLYSACCHARIDE

Changsuk Moon[1], Hyun-Jeong Park[1], Youn-Hee Choi[1], Eun-Mi Park[2], Vincent Castranova[3], Jihee Lee Kang[1]

[1]Departments of Physiology
[2]Pharmacology, Division of Cell Biology, Ewha Medical Research Center, School of Medicine, Ewha Woman's University, Seoul, South Korea
[3]Pathology and Physiology Research Branch, Health Effects Laboratory Division, National Institute for Occupational Safety and Health, Morgantown, West Virginia, USA

Nanoparticles are widely used in nanomedicines, including for targeted delivery of pharmacological, therapeutic, and diagnostic agents. Since nanoparticles might translocate across cellular barriers from the circulation into targeted organs, it is important to obtain information concerning the pathophysiologic effects of these particles through systemic migration. In the present study, acute pulmonary responses were examined after intraperitoneal (ip) administration of ultrafine titanium dioxide (TiO$_2$, 40 mg/kg) in mice at rest or in lungs primed with lipopolysaccharide (LPS, ip, 5 mg/kg). Ultrafine TiO$_2$ exposure increased neutrophil influx, protein levels in bronchoalveolar lavage (BAL) fluid, and reactive oxygen species (ROS) activity of BAL cells 4 h after exposure. Concomitantly, the levels of proinflammatory mediators, such as tumor necrosis factor (TNF)-α, interleukin (IL)-1β, and macrophage inflammatory protein (MIP)-2 in BAL fluid and mRNA expression of TNF-α and IL-1β in lung tissue were elevated post ultrafine TiO$_2$ exposure. Ultrafine TiO$_2$ exposure resulted in significant activation of inflammatory signaling molecules, such as c-Src and p38 MAP kinase, in lung tissue and alveolar macrophages, and the nuclear factor (NF)-κB pathway in pulmonary tissue. Furthermore, ultrafine TiO$_2$ additively enhanced these inflammatory parameters and this signaling pathway in lungs primed with lipopolysaccharide (LPS). Contrary to this trend, a synergistic effect was found for TNF-α at the level of protein and mRNA expression. These results suggest that ultrafine TiO$_2$ (P25) induces acute lung inflammation after ip administration, and exhibits additive or synergistic effects with LPS, at least partly, via activation of oxidant-dependent inflammatory signaling and the NF-κB pathway, leading to increased production of proinflammatory mediators.

Ultrafine titanium dioxide (TiO$_2$), one type of manufactured nanoparticle that is being produced in tons each year, is found in white paint, paper, ceramics, plastics, consumer products (e.g., sunscreens and cosmetics), and photocatalysts to purify air and water. Most of the toxicity research on nanoparticles *in vivo* has been carried out in laboratory animals with a focus on respiratory-system exposures to assess significant adverse health effects, because it is a potential portal of entry for airborne ultrafine particles (Oberdörster et al., 2005). The results of several prolonged inhalation exposure studies on rodents demonstrated

that high levels of ultrafine TiO$_2$ (2–10 mg/kg) produced inflammation, pulmonary damage, fibrosis, and lung tumors (Bermudez et al., 2004; Warheit et al., 2006). Renwick et al. (2004) reported that acute toxicity of intratracheal (i.t.) instillation of ultrafine TiO$_2$ (1 mg/kg) on lung epithelium was associated with development of inflammation and increased chemotactic activity of alveolar macrophages. Furthermore, a significant portion of inhaled ultrafine TiO$_2$ may migrate into the alveolar interstitium and pulmonary capillaries within 24 h of lung deposition (Muhlfeld et al., 2007; Oberdörster et al., 2005).

Nanosized TiO$_2$ has potential applications in nanomedicine for molecular imaging, diagnosis, drug delivery, anticancer therapy, and gene therapy, although it was reported to produce pulmonary toxicity after i.t. inhalation or instillation. Recently, TiO$_2$ nanoparticles were proposed as a suitable method of delivering drugs to tissue or cells (Lopez et al., 2006, 2007; Ayon et al., 2006; Xu et al., 2007). López et al. (2008) reported using TiO$_2$ nanoparticle carriers (approximately 40–50 mg/kg) in animal models to test therapeutic effects on brain tumors.

Titanium is widely used in the manufacture of odontological and orthopedic implants. Thus, recent investigations were undertaken to obtain information on the biological responses and toxicity and to gain insight into targets of intravenously (iv) or orally administered ultrafine TiO$_2$. Fabian et al. (2008) found that in rats exposed to ultrafine TiO$_2$ (5 mg/kg body weight) by a single iv injection showed peak TiO$_2$ levels at d 1 in liver, spleen, lung, and kidneys with no apparent adverse health effects. In contrast, ultrafine TiO$_2$ administered at a much higher dose (5 g/kg) to mice by a single oral gavage (Wang et al., 2007) resulted in hepatic and kidney dysfunction. Several studies from Olmedo et al. (2008a, 2008b) demonstrated that at 6 mo postinjection (16 g/kg, ip), TiO$_2$ (1 μm in diameter) was present in all organs examined through systemic migration in rats. However, little is known about acute lung reactions following systemic exposure to ultrafine TiO$_2$ at an appropriate therapeutic dose range.

Acute and chronic exposure to increased ambient amounts of particulate matter (PM) is associated with an increase in morbidity and mortality for cardiopulmonary conditions (Dockery & Pope, 1994; Pope et al., 1995a; Schwartz et al., 1996; Krewski et al., 2005). One intriguing aspect of the epidemiological data is that adverse health effects are primarily seen in people with preexisting inflammatory lung disease (Pope et al., 1995b; Schwartz, 1994). A plausible biologic mechanism linking short-term particle exposure and pathophysiologic effects has not been elucidated. In the present study, acute toxicity of ultrafine TiO$_2$ was examined on the lung after ip administration (40 mg/kg). Furthermore, pulmonary responses to ultrafine TiO$_2$ in lungs primed by lipopolysaccharide (LPS) were also determined. In particular, the effects of ip exposure to ultrafine TiO$_2$ were determined on inflammatory signaling pathways and transcription factor activation in lungs both in the absence and presence of LPS.

METHODS

Reagents

Lipopolysaccharide (LPS; *Escherichia coli* lipopolysaccharide, 055:B5) was purchased from Sigma Chemical Company (St. Louis, MO). The antibodies used in this study were rabbit anti-phospho-c-Src (pY418), anti-c-Src, anti-rabbit phospho-p38 MAP kinase/p38 MAP kinase, anti-IκB-α rabbit polyclonal, and antiphospho-IκB-α (Serine 32) (New England Biolabs, Inc., Beverly, MA).

Particle Sieving and Suspension

Ultrafine titanium dioxide (Aeroxide TiO$_2$ P-25, 80% anatase and 20% rutile, primary particle diameter of 21 nm) was obtained as a gift from the Degussa Corporation (Parsippany, NJ). The surface area of the ultrafine TiO$_2$ sample, determined by BET (Brunauer, Emmett, and Teller) gas absorption, was 48.08 m^2/g (Sager et al., 2008). The particulate sample was sieved in a Retsch AS 200 sieve (Retsch GmbH, Haan, Germany) at a vibration amplitude of

50 for 15 min to break apart large clumps. Three different sieve sizes (1.18 mm, 250 μm, 45 μm openings) were used successively in the sieving process.

Prior to suspension, the particle samples were sterilized by heating at 160°C for 90 min in a dry oven. The particles were suspended in Ca^{+2}- and Mg^{+2}-free phosphate-buffered saline (PBS) containing 10 μg/ml dipalmitoyl phosphatidylcholine (DPPC) plus 0.6 mg/ml bovine serum albumin (BSA). DPPC was prepared as a 10 mg/ml stock solution in absolute ethanol. Thus, the final concentration of ethanol in the dispersion medium was 0.1 % (v/v) (Sager et al., 2007). Electron microscopic evaluation of such suspension indicates that the majority of TiO_2 structures were in the 200–300 nm range (Sager et al., 2008). Pulmonary exposure to the dispersion medium did not affect baseline lung reactions (Sager et al., 2007).

Animal Protocols

Specific-pathogen-free male BALB/c mice (Daehan Biolink Co. Eumsung-Gun, Chungbuk, Republic of Korea) weighing 19–21 g were used in all experiments. The Ethics Review Committee for Animal Experimentation of Ewha Woman's University School of Medicine approved the experimental protocol. Mice were cared for and handled in accordance with the National Institutes of Health (NIH) Guide for the Care and Use of Laboratory Animals.

Mice were divided into four experimental groups. The vehicle group was injected ip in 200 μl sterile PBS. The nanoparticle group was injected ip with a suspension of ultrafine TiO_2 (40 mg/kg body weight). The LPS group was injected ip with LPS (5 mg/kg) dissolved in vehicle as described for lung injury models (Severgnini et al., 2005). The LPS and nanoparticle group was injected ip with a suspension of ultrafine TiO_2 (40 mg/kg body weight) 30 min after the LPS injection (5 mg/kg). Mice revived unassisted after approximately 10–20 min. Animals were sacrificed at 4 h after TiO_2, and the following parameters were monitored: (1) cell differential and protein content in bronchoalveolar lavage (BAL) fluid; (2) oxidant production in BAL cells; (3) mRNA expression and protein levels of proinflammatory mediators in lung tissue and BAL fluid, respectively; (4) activation of inflammatory signaling molecules, such as c-SRC and p38 MAP kinase, in lung tissue; and (5) activation of nuclear factor-κB (NF-κB) and activator protein-1 (AP-1) in lung tissue.

Isolation of Bronchoalveolar Lavage (BAL) Cells, Lung Tissue, and Cell Counts

Mice were anesthetized with a mixture of ketamine and xylazine (200 and 10 mg/kg, ip, respectively) and exsanguinated by cutting the descending aorta. Bronchoalveolar lavage (BAL) was performed through a tracheal cannula using 0.8-ml aliquots of ice-cold Ca^{2+}/Mg^{2+}-free phosphate-buffered medium (145 mM NaCl, 5 mM KCl, 1.9 mM NaH_2PO_4, 9.35 mM Na_2HPO_4, and 5.5 mM dextrose; pH 7.4) to a total of 2.4 ml for each mouse. BAL samples so obtained were centrifuged at 500 × g for 5 min at 4°C, and cell pellets were washed and resuspended in phosphate-buffered medium. Cell counts were determined using an electronic Coulter Counter fitted with a cell sizing analyzer (Coulter model ZBI with a channelizer 256; Coulter Electronics, Bedfordshire, UK), as described by Lane and Mehta (1990). Neutrophils and alveolar macrophages were identified by their characteristic of cell diameter (Castranova et al., 1990). Cytospin preparations of BAL cells were stained with a modified Wright–Giemsa stain (VWR, Boston) to identify alveolar macrophages loaded with TiO_2 particles (Huynh et al., 2005). Recovered cells were 98% viable, as determined by trypan blue dye exclusion. After BAL, lungs were removed, immediately frozen in liquid nitrogen, and stored at –70°C.

Cell Culture

Alveolar macrophages from each animal group were isolated by adhesion (60 min) and cultured in serum-free X-vivo 10. Murine RAW 264.7 macrophages (American type Culture Collection [ATCC]) were cultured in Dulbecco's

modified Eagle's medium (DMEM) supplemented with 5% heat-inactivated fetal bovine serum (HyClone, Logan, UT), 2 mM L-glutamine, 100 µg/ml streptomycin, and 100 U/ml penicilline in humidified 10% CO$_2$ at 37°C. Cells from passages 7 and 8 only were used in particle experiments.

Measurement of Total Protein

BAL sample protein concentration was used as an indicator of air/blood barrier integrity. Total protein was measured using supernatants from the first BAL fluid samples according to the method of Hartree (1972), using bovine serum albumin (BSA) as a standard.

Measurement of Intracellular ROS Generation

BAL cells (2.5 × 10^5 cells/well) were stained with 10 µM H$_2$DCF-DA (2′,7′-dichlorofluorescein diacetate) in PBS for 30 min at 37°C. DCF fluorescence intensity was measured at 488 nm excitation and at 525 nm emission using a fluorescence microplate reader (Molecular Devices, CA).

Measurement of TNF-α, IL-1β, and MIP-2

Supernatants from the first BAL fluid samples were assayed using tumor necrosis factor (TNF)-α, interleukin (IL)-1β, and macrophage inflammatory protein (MIP)-2 (BioSource International, Camarillo, CA) enzyme-linked immunosorbent assay (ELISA) kits (R &D Systems, Minneapolis, MN) according to the manufacturer's instructions.

RNA Isolation and RT-PCR

Total RNA was isolated from lung homogenates using TRIzol reagent (Invitrogen Life Technologies, Carlsbad, CA). The concentration and purity of RNA were evaluated by spectrometry at 260 and 280 nm. Reverse transcription was conducted for 60 min at 42°C with 1 µg of total RNA using Power cDNA Synthesis kit (Intron Biotechnology, Seoul, Korea). TNF-α and IL-1β mRNA levels were determined using relative quantitative PCR kit (Intron Biotechnology). The sequences of the primers used for the PCR were as follows: TNF-α (sense 5′-GAA CTG GCA GAA GAG GCA CTC-3′ and anti-sense 5′-AGG GTC TGG GCC ATA GAA CTG-3′), IL-1β (sense 5′-TCG CTC AGG GTC ACA AGA AA-3′ and anti-sense 5′-ATC AGA GGC AAG GAG GAA ACA C-3′), and β-actin (sense 5′-GAT GAC GAT ATC GCT GCG CTG-3′ and anti-sense 5′-GTA CGA CCA GAG GCA TAC AGG-3′). The cDNA was denatured for 5 min at 94°C, and the amplification was achieved in a temperature cycler (Perkin Elmer GeneAmp PCR System 2400, Waltham, MA) by 30 cycles of temperature (94°C for 30 s, 54 °C for 30 s, 72°C for 30 s), followed by a 7-min final extension at 72°C. A total of 5 µl of each PCR sample was loaded on a 1.5% agarose gel stained with ethidium bromide. The relative densities of the cytokine vs β-actin were analyzed by densitometry.

Western Blot Analysis

Lung tissue homogenate and cell lysate samples (50 µg protein/lane) were separated on 10% sodium dodecyl sulfate (SDS)–polyacrylamide gels. Separated proteins were electrophoretically transferred onto nitrocellulose paper and blocked for 1 h at room temperature with Tris-buffered saline containing 3% bovine serum albumin (BSA). Membranes were then incubated with the indicated antibody and visualized by enhanced chemiluminescence (ECL).

Nuclear Extracts

Nuclear extracts were prepared using a modification of the method described by Lee et al. (2007). Nuclear extracts were prepared from lung tissue samples. Aliquots of frozen tissue were placed in a Precellys tissue homogenizer (Bertin Technol., Cedex, France), containing 0.5 ml buffer A (100 mM HEPES, pH 7.9, 10 mM KCl, 0.1 M ethylenediamine tetraacetic acid [EDTA], 0.5 mM dithiothreitol [DTT], 0.6% Nonidet P-40, and 0.5 mM phenylmethylsulfonyl fluoride [PMSF]) to lyse cells. Supernatants containing intact nuclei were incubated on ice for 5 min and centrifuged for 10 min at 5000 rpm. Nuclear pellets were resuspended in buffer C (20 mM HEPES, pH

7.9, 20% glycerol, 0.42 M NaCl, 1 mM EDTA, and 0.5 mM PMSF) for 30 min on ice. The supernatants, which contained nuclear proteins, were collected by centrifuging at 8500 × g for 2 min and stored at –70°C.

Electrophoretic Mobility Shift Assay (EMSA)

Binding reaction mixtures (10 µl), containing 5 µg (4 µl) of nuclear extract protein, 2 µg poly (dI-dC)·poly (dI-dC) (Sigma Co., St. Louis. MO), and 40,000 cpm ^{32}P-labeled probe in binding buffer (4 mM HEPES, pH 7.9, 1 mM MgCl$_2$, 0.5 mM DTT, 2% glycerol, and 20 mM NaCl) were incubated for 30 min at room temperature. Protein–DNA complexes were separated on 5% non-denaturing polyacrylamide gels in 1 × TBE buffer and autoradiographed. Autoradiograph signals of activated nuclear factor (NF)-κB or activator protein (AP)-1 were quantitated by densitometry using an UltroScan XL laser densitometer (LKB, model 2222-020, Bromma, Sweden) to determine band intensities.

The oligonucleotide used as a probe for electrophoretic mobility shift assay (EMSA) was a double-stranded DNA fragment, containing the NF-κB (5′-CCTGTGCTCCG GGAATTTC CCTGGCC-3′) and AP-1 (5′-CTGCGCTTGAT GACTCAGCAGCCCGGA-3′) consensus sequence and labeled with [α-^{32}P]-dATP

(Amersham, Buckinghamshire, UK) using DNA polymerase Klenow fragment (Life Technologies, Gaithersburg, MD). Cold competition and nonspecific binding were performed by adding 100 ng unlabeled double-stranded probe to reaction mixtures.

Statistical Analysis

Values are expressed as means ± standard errors. Intergroup comparisons were made using one-way analysis of variance (ANOVA) followed by Tukey's post hoc test. Statistical significance was accepted for p values <.05.

RESULTS

Effects of Ultrafine TiO$_2$ on BAL Protein and Inflammatory Cell Yield

To evaluate the magnitude of pulmonary inflammation, recruitment of inflammatory cells into lungs was determined 4 h after ip administration of ultrafine TiO$_2$ (Figure 1A). Ultrafine TiO$_2$ alone significantly increased neutrophil numbers in BAL fluid 2.2-fold. As expected, ip LPS exposure significantly elevated the number 2.9 fold. When ultrafine TiO$_2$ was administered 30 min after LPS exposure (the LPS + nanoparticle group), neutrophil numbers were increased 4.9-fold, which was not significantly different from the sum of
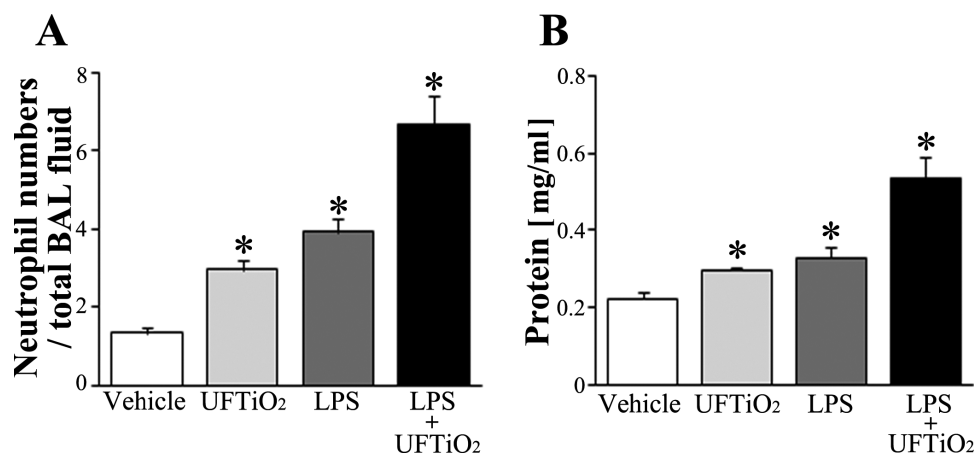
FIGURE 1. Effects of ip administered ultrafine TiO$_2$ on BAL inflammatory cell yields and protein accumulation in BAL fluid. Mice were administered ip vehicle, ultrafine TiO$_2$ (40 mg/kg), LPS (5 mg/kg), or ultrafine TiO$_2$ (40 mg/kg) 30 min after LPS (5 mg/kg), and were sacrificed at 4 h post TiO$_2$. Values represent means ± SEM of 10 mice per group. Asterisk indicates significantly different from the vehicle group, p < .05.

effects of separate treatment with nanoparticles or LPS. Alveolar macrophage numbers were not affected 4 h after these stimulants were administered alone or together compared with vehicle (data not shown).

Protein accumulation in BAL fluid 4 h after ip administration of ultrafine TiO_2, as an indicator of air/blood barrier integrity is shown in Figure 1B. Exposure to nanoparticles or LPS significantly enhanced protein levels in BAL fluid by 1.3- and 1.5-fold, respectively. The protein levels in the LPS + nanoparticle group were increased by 2.4-fold compared with vehicle, but this level was not significantly greater than the sum of responses in the nanoparticle or LPS individually.

Effects of Ultrafine TiO₂ on Oxidant Generation by BAL Cells

To investigate the contribution of oxidative stress after ip exposure to ultrafine TiO_2, intracellular oxidant generation by BAL cells was examined using the DCF-DA probe. Ultrafine TiO_2 enhanced ROS generation 1.7-fold and the values were comparable to those of LPS-exposed mice (Figure 2). Furthermore, The ROS levels in the LPS + nanoparticle group were increased by 3.2-fold compared with control. This latter level was not significantly greater than the sum of responses in nanoparticle or LPS alone.

Effects of Ultrafine TiO₂ on Protein Levels and mRNA Expression of Proinflammatory Mediators in Lung Tissue

Tumor necrosis factor (TNF)-α, interleukin (IL)-1β, and macrophage inflammatory protein (MIP)-2 are representative proinflammatory mediators that play major roles in neutrophil influx and lung damage. The nanoparticles increased protein levels of TNF-α, IL-1β, and MIP-2 by 2.3-, 1.8-, and 1.8-fold, respectively (Figure 3, A, B, and C). As expected, LPS exposure significantly elevated protein levels (TNF-α, IL-1β, and MIP-2) 4.3-, 2.1-, and 3.3-fold. These mediator levels in the LPS + nanoparticle group were increased by 14-, 3.1-, and
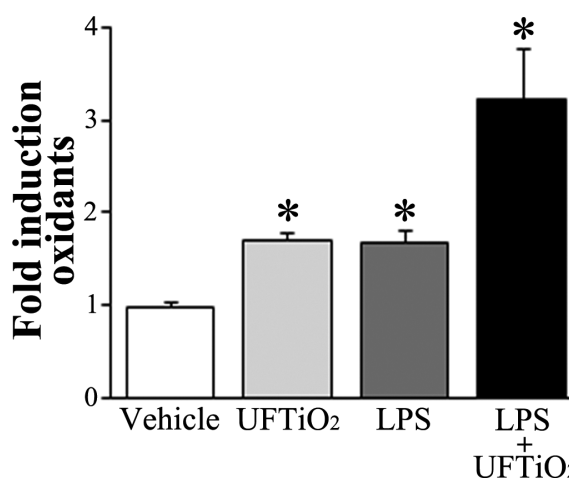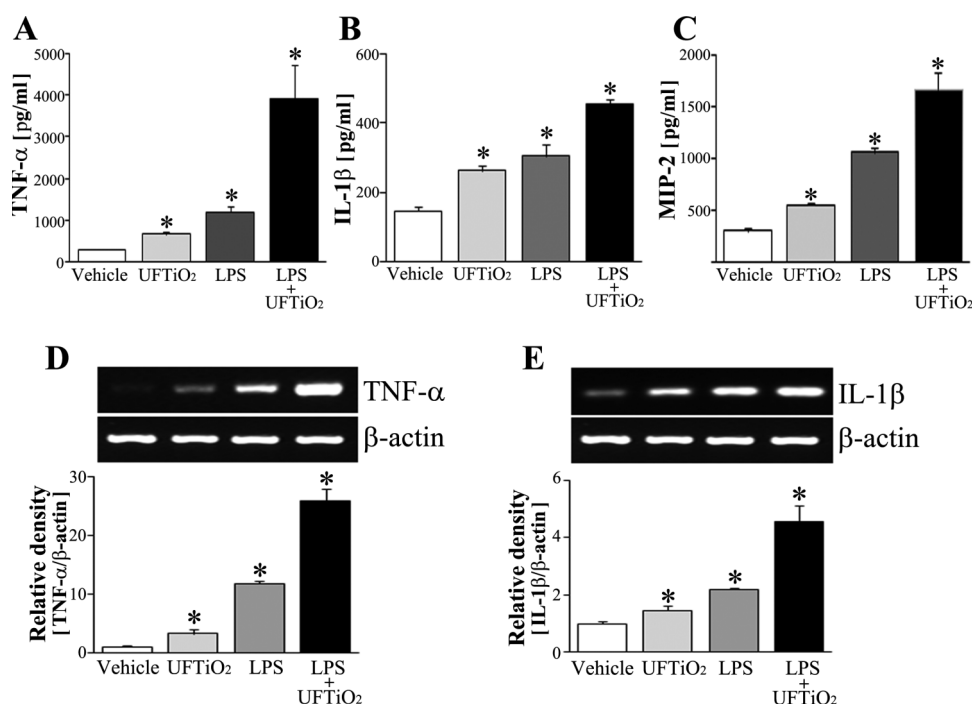

FIGURE 2. Effects of ip administered ultrafine TiO_2 on oxidant generation by BAL cells. Mice were administered ip vehicle, ultrafine TiO_2 (40 mg/kg), LPS (5 mg/kg), or ultrafine TiO_2 (40 mg/kg) 30 min after LPS (5 mg/kg), and were sacrificed at 4 h post TiO_2. BAL cells were incubated with H_2DCFH-DA for 30 min at rest. DCF fluorescence intensity was measured using a fluorescence microplate reader. Increases in intracellular ROS are expressed as fold induction over the vehicle. Values represent means ± SEM of 10 mice per group. Asterisk indicates significantly different from the vehicle group, $p < .05$.

4.5-fold, respectively, compared with vehicle. For IL-1β and MIP-2, the responses to combined exposures did not differ significantly from the sum of the individual responses.

To determine whether the enhancement occurred at the level of transcription, quantitative reverse-transcription polymerase chain reaction (RT-PCR) was used to determine mRNA expression of proinflammatory cytokines, TNF-α and IL-1β, in lung tissue. LPS exposure markedly increased steady-state mRNA expression for TNF-α (Figure 3D) and IL-1β (Figure 3E) compared with vehicle. Ultrafine TiO_2 exposure produced a significant rise in the mRNA expression for both cytokines. These mRNA levels in the LPS + nanoparticle group were further increased after combined exposures to nanoparticles and LPS.

Effects of Ultrafine TiO₂ on Activation of Inflammatory Signaling Molecules

Since ultrafine TiO_2 elevated oxidant generation in BAL cells and inflammatory mediator production at both the mRNA and protein levels, it was important to determine
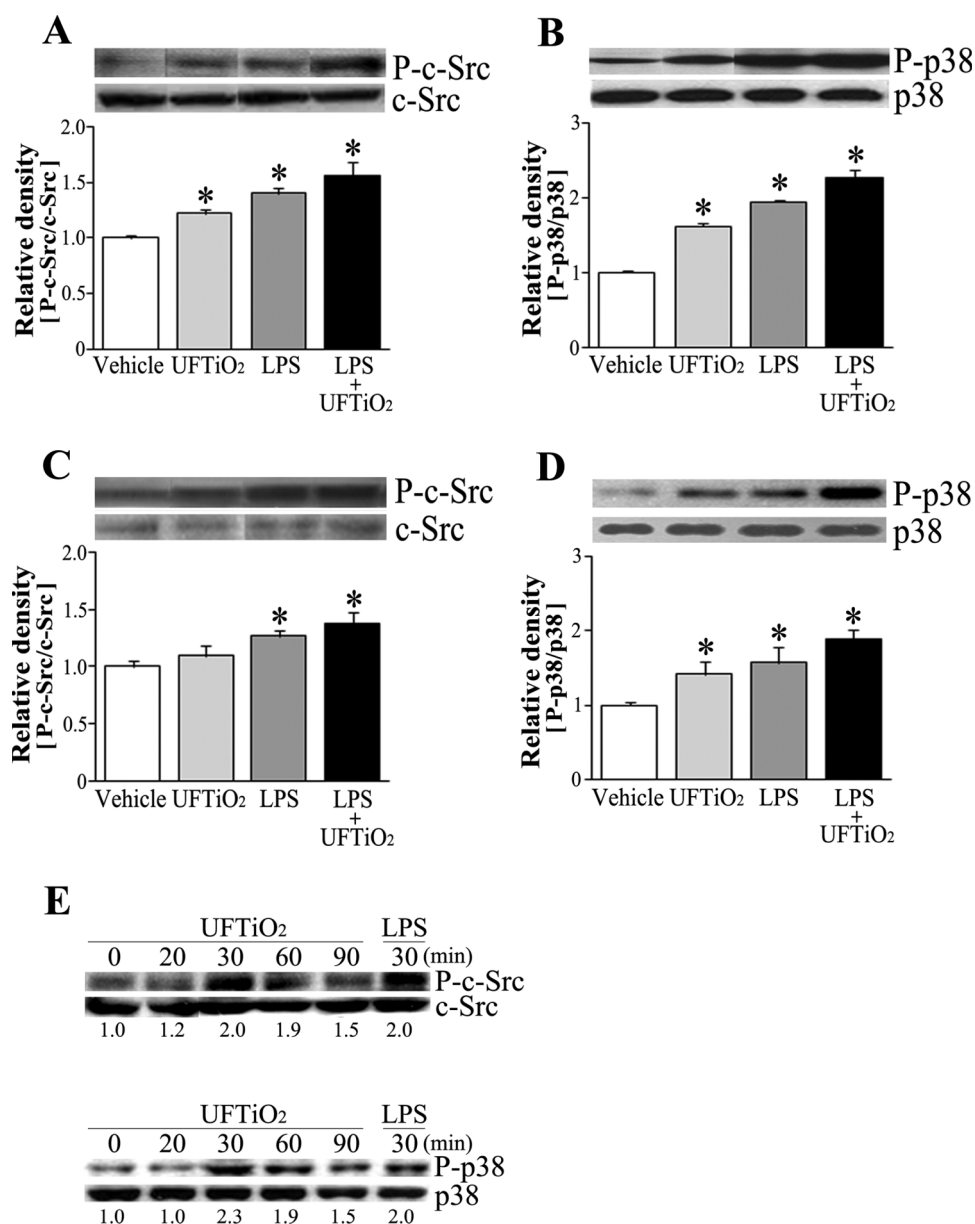
FIGURE 3. Effects of ip administered ultrafine TiO$_2$ on protein levels and mRNA expression of pro-inflammatory mediators. Mice were administered ip vehicle, ultrafine TiO$_2$ (40 mg/kg), LPS (5 mg/kg), or ultrafine TiO$_2$ (40 mg/kg) 30 min after LPS (5 mg/kg), and were sacrificed at 4 h post TiO$_2$. Protein levels of TNF-α (A) L-1β (B), and MIP-2 (C) in BAL fluid samples were quantified using enzyme-linked immunosorbent assays. mRNA expression of TNF-α(D) and IL-1β (E) was measured in lung tissue. For quantification, PCR bands in photographs of the gel were scanned by a densitometer linked to a computer analysis system. Reverse transcription polymerase chain reaction technique was used to measure relative differences in transcript amounts after normalization versus amounts of the reference gene β-actin. Values represent means ± SEM of 10 mice per group. Asterisk indicates significantly different from the vehicle group, $p < .05$.

whether this is regulated by oxidant-dependent signaling. The c-Src tyrosine kinase (TK) and p38 mitogen-activated protein (MAP) kinase play key roles in oxidant-mediated signal transduction and proinflammatory mediator production during acute lung injury (Ding et al., 1999; Khadaroo et al., 2003; Kim et al., 2006; Lee et al., 2007; Nishida et al., 2000). Thus, phosphorylation of c-Src and p38 MAP kinase was studied in lung tissue and alveolar macrophages 4 h after ip administration of ultrafine TiO$_2$ or LPS. LPS exposure resulted in marked increases in phosphorylation of these molecules in lung tissue and alveolar macrophages. Ultrafine TiO$_2$ enhanced the phosphorylation of c-Src and p38 MAP kinase in lung tissue (Figure 4, A and B) and p38 MAP kinase in alveolar macrophages (Figure 4, C and D). The effects of ultrafine TiO$_2$ on phosphorylation of these kinases were also observed following *in vitro* exposure (Figure 4E), where phosphorylated c-Src and p38 MAP kinase levels in RAW 264.7 macrophages peaked 30 min after exposure to ultrafine TiO$_2$ (0.5 μg/ml) and then declined up to 90 min following exposure. Phosphorylation levels of both kinases in the LPS + ultrafine TiO$_2$ group in lung tissue and alveolar macrophages were not significantly different from the sum of the responses to LPS or nanoparticles alone.

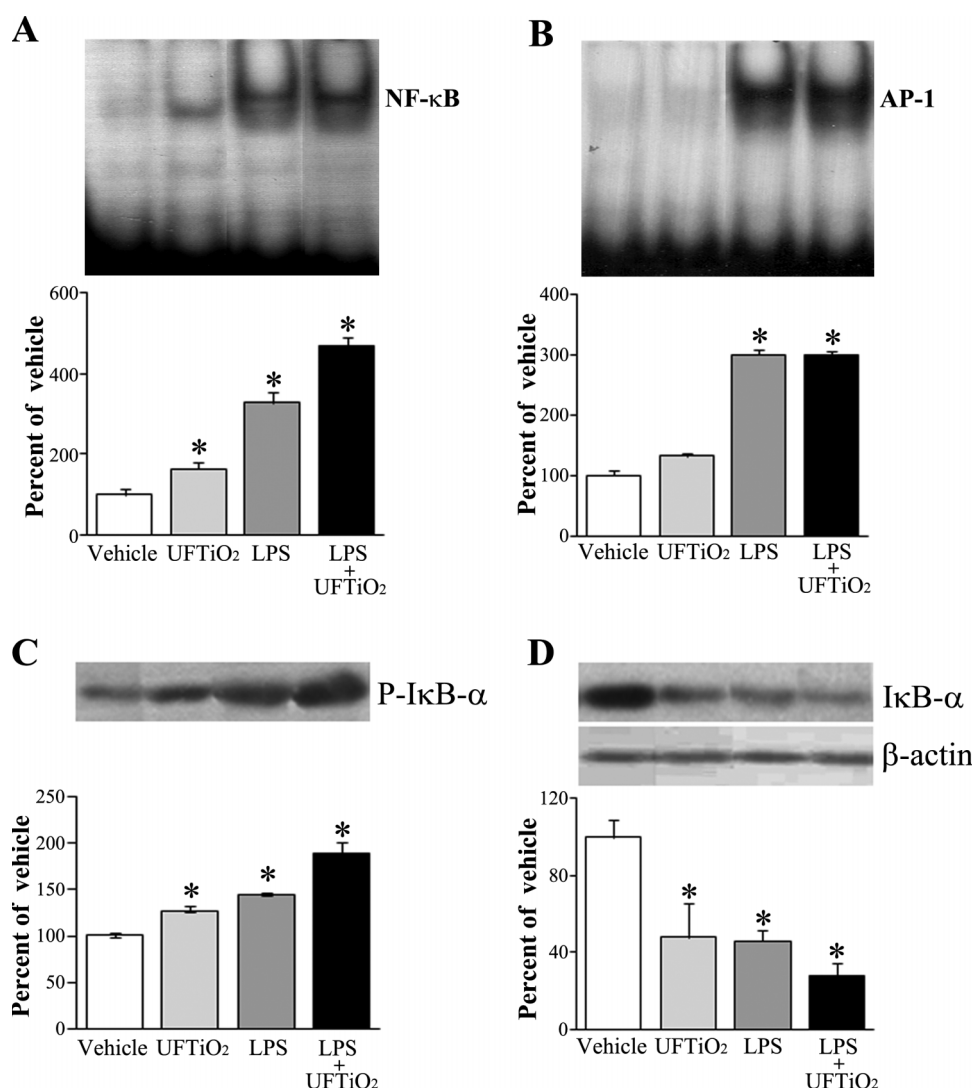### Effects of Ultrafine TiO$_2$ on Activation of NF-κB and AP-1 in Lung Tissue

The genes that encode many inflammatory mediators, such as TNF-α, IL-1β, and MIP-2, are under the control of the oxidant-sensitive inflammation-related transcription factors NF-κB and AP-1 (Drouet et al., 1991; Rhoades et al., 1992). Src TKs and MAP kinase signaling pathways were correlated with activation of

FIGURE 4. Effects of ultrafine TiO$_2$ on phosphorylation of c-Src and p38 MAP kinase in lung tissue (A, B), alveolar macrophages (C, D) and RAW 264.7 macrophages (E). Mice were administered ip vehicle, ultrafine TiO$_2$ (40 mg/kg), LPS (5 mg/kg), or ultrafine TiO$_2$ (40 mg/kg) 30 min after LPS (5 mg/kg), and were sacrificed at 4 h post TiO$_2$ (A-D). Western blotting with each anti-specific (phospho) c-Src or p38 MAP kinase Ab was performed on lung tissue homogenates and cell lysates. Relative values for the phosphorylated signaling molecule versus the corresponding are indicated below the gel. Values represent means ± SEM of five mice per group (A, B) or three independent experiments in alveolar macrophages from two or three mice per group (C, D). Asterisk indicates significantly different from the vehicle group, $p < .05$. (E) Results are representative results.

these transcription factors (Lee et al., 2007; Kang et al., 2006; Kim et al., 2006; Shaulian & Karin, 2002). In the present study, phosphorylation of c-Src and p38 MAP kinase occurred after ultrafine TiO$_2$ exposure. Further, DNA binding activities of NF-κB and AP-1 were markedly elevated in lung tissue after LPS exposure. Ultrafine TiO$_2$ exposure resulted in a significant rise in NF-κB activation (Figure 5A), while the increase in AP-1 activation was not significant (Figure 5B). Ultrafine TiO$_2$ increased phosphorylation (Figure 5C) and degradation (Figure 5D) of IκB-α in lung

FIGURE 5. Effects of ip administered ultrafine TiO_2 on activation of NF-κB and AP-1. Mice were administered ip vehicle, ultrafine TiO_2 (40 mg/kg), LPS (5 mg/kg), or ultrafine TiO_2 30 min after LPS (5 mg/kg), and were sacrificed at 4 h post TiO_2. Nuclear extracts were prepared from lung tissue. Densities of NF-κB (A) and AP-1 (B) bands on EMSA are expressed as percentage of vehicle controls. Western blots with anti-serine phospho IκB-α (Ser32) (C) and IκB-α (D) in lung lysates. Densities are expressed as percentages of the vehicle group. Values represent means ± SEM of five mice per group. Asterisk indicates significantly different from the vehicle group, $p < .05$.

tissue. NF-κB activation and phosphorylation and degradation of IκB-α in lungs of the ultrafine TiO_2 + LPS group were not significantly different from the sum of the individual effects of LPS or nanoparticles. These activities were specific for NF-κB or AP-1, since the addition of the cold competitor for each transcription factor eliminated specific bands in each samples for the LPS or/and ultrafine TiO_2 group, but the addition of the nonspecific competitor did not (data not shown).

Alveolar Macrophages Were Loaded With Particles

To verify translocation of ultrafine TiO_2 to lung after ip administration, cytospins of BAL cells were conducted from the nanoparticle and LPS + nanoparticle group and microscopically examined. Alveolar macrophages containing particles in their cytoplasm were clearly identified in both groups (Figure 6 A). Furthermore, the percentage of cells containing
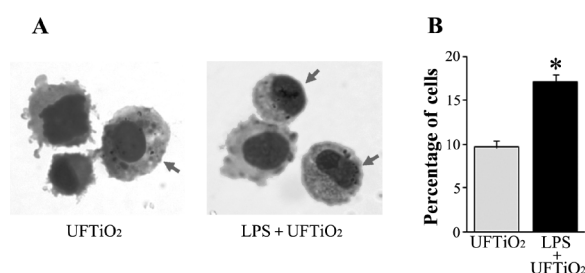
FIGURE 6. Alveolar macrophages containing particles after ip exposure. Mice were administered ip vehicle, ultrafine TiO$_2$ (40 mg/kg) at rest, or were administered ip ultrafine TiO$_2$ (40 mg/kg) 30 min after LPS (5 mg/kg), and were sacrificed at 4 h post TiO$_2$. (A) Note the presence of BAL cytospin alveolar macrophages containing particles. (B) Percentages of cells containing particles per 200 alveolar macrophages in light microscopic field. Asterisk indicates significantly different between levels of the LPS + ultrafine TiO$_2$ group and the ultrafine TiO$_2$ group, $p < .05$.

particles per 200 alveolar macrophages in light-microscopic fields from the LPS + nanoparticle group was 1.8-fold greater than in nanoparticle group (Figure 6B). These findings indicate that ultrafine TiO$_2$ administered ip by the systemic route migrates and translocates to the lung across the blood–air barrier and that this translocation of particles is enhanced by LPS.

DISCUSSION

This is the first study to demonstrate acute lung inflammatory responses to ultrafine TiO$_2$ following ip administration. A second novel observation in the present study is that ultrafine TiO$_2$ exhibits additivity in lungs primed by LPS. TiO$_2$ particles are not only transported in blood by cells, but also transported by plasma (Urban et al., 2000). Indeed, our cytospin findings indicated that ultrafine TiO$_2$ administered systemically migrated to the lung across the blood–air barrier and were engulfed by alveolar macrophages. There was no detectable inflammatory response or organ toxicity in the lung, liver, spleen, and kidneys on d 1 after iv treatment of rats with ultrafine TiO$_2$ (5 mg/kg) (Fabian et al., 2008). In contrast, nanosized TiO$_2$ administered orally to mice at a single much higher dose (5 g/kg body weight) produced changes in serum biochemical parameters (alanine aminotransferase/

aspartate aminotransferase [ALT/AST], lactate dehydrogenase [LDH]) and pathology, indicating hepatic injury in 2 wk (Wang et al., 2007). In the same study, increased blood urea nitrogen (BUN) and renal pathological changes were also observed in the treated animals. In addition, significant increases in serum LDH and alpha-hydroxybutyrate dehydrogenase (HBDH) suggested myocardial damage. Warheit et al. (2007) reported similar evidence of organ and tissue damage or dysfunction 48 h after an oral dose of 175, 550, or 1750 mg/kg given to rats. However, there are no reports indicating acute toxicity of ultrafine TiO$_2$ to lung after iv or ip administration. Using a dose of TiO$_2$ nanoparticles adapted from animal models for the development as drug carriers (López et al., 2008), particles were injected ip into mice at a dose of 40 mg/kg in the current study. Lung inflammatory responses were shown 4 h postexposure, as demonstrated by significant increases in neutrophil influx and protein accumulation in BAL fluid. The difference between the results regarding lung toxicity in our current study and those of Fabien et al. (2008) seems to be related to the higher dose (eightfold), although it cannot be excluded that different experimental animal species used (mice vs. rats) or the samples analyzed (BAL fluid vs serum samples), or the exposure routes (ip vs. iv) may account for differences between these studies.

Previously, Kang et al. (2008) demonstrated that *in vitro* exposure of RAW 264.7 macrophages to ultrafine TiO$_2$ exerted significant biological activity as measured by reactive oxygen species (ROS) generation and proinflammatory mediator (TNF-α and MIP-2) secretion. Recently, Monteiller et al. (2007) noted that IL-8 protein release and glutathione (GSH) depletion in human alveolar epithelial type II-like cells predicted pro-inflammatory effects and oxidative stress after *in vivo* treatment with ultrafine TiO$_2$. Consistent with this study, the present investigation reported that ultrafine TiO$_2$ increased ROS generation in BAL cells and proinflammatory mediator (TNF-α, IL-1β, and MIP-2) production in BAL fluid. Interestingly, oxidant generation by BAL cells in the

nanoparticle group was comparable to the LPS group. The elevation of mRNA levels for TNF-α and IL-1β in lung tissue indicates that enhancement occurred at the level of transcription. Since the increases in production of these mediators and ROS were associated with neutrophil influx and lung injury (Blackwell et al., 1996; Kristof et al., 1998), these factors may play an important role in ultrafine TiO$_2$-induced lung inflammation. Although the precise mechanisms through which ip injected particles exert biological effects on lungs are unknown, it is possible that direct passage of nanoparticles to the lung rather than systemic inflammatory effects may be involved, since ultrafine TiO$_2$ did not induce significant alterations in TNF-α and MIP-2 levels in serum 4 h postexposure (data not shown).

To date, there have been few data elucidating molecular mechanisms related to inflammatory responses to ultrafine TiO$_2$ exposure. In the current study, the inflammatory signaling cascades involving activation of c-Src and p38 MAP kinase were noted in lung and alveolar macrophages after exposure to ultrafine TiO$_2$. Activation of these kinases and ERK (Kang et al., 2008) in RAW 264.7 macrophages was also found after *in vitro* exposure to ultrafine TiO$_2$. These *in vivo* and *in vitro* data also support the concept that ultrafine TiO$_2$ acts directly following passage after systemic exposure to affect these signaling pathways in alveolar macrophages. Further, ultrafine TiO$_2$ induced activation of NF-κB through phosphorylation and degradation of IκB-α. However, activation of AP-1 was less striking at this time point. The Src family tyrosine kinases were shown to play key roles in oxidant-mediated signal transduction in lymphocytes and macrophages (Khadaroo et al. 2003; Nishida et al., 2000). The c-Src activation is required for phosphorylation of IκB-α and NF-κB activation in macrophages stimulated with TNF-α, silica, or LPS (Abu-Amer et al., 1998; Kang et al., 2005, 2006). Another group of oxidant-dependent signaling molecules potentially important in inflammation is the MAP kinases. Friedland et al. (2001) reported that p38 MAP kinase regulates NF-κB-driven

gene expression, in part, by increasing the association of the basal transcription factor, TATA-binding protein with the p65 subunit of NF-κB. Previously, Lee et al. (2007) demonstrated that PP1 and SB203580, a specific inhibitor of Src TK and p38 MAP kinase (Kim et al., 2006), respectively, blocked the phosphorylation and degradation of IκB-α, and the DNA binding activity of NF-κB in the lung 4 h after LPS instillation. Data thus indicated that Src TK and p38 MAP kinase play important roles in the induction of NF-κB pathway *in vivo*. Taken together, elucidating mechanisms for the ultrafine TiO$_2$-induced inflammatory signaling cascades leading to NF-κB activation associated with oxidative stress is of basic importance.

Circulating endotoxin was linked to the development of acute lung injury in critically ill patients and experimentally following systemic exposure (Denis et al., 1994). In our experimental model, ultrafine TiO$_2$ was administered 30 min after LPS exposure to mimic the context of the already primed lung by LPS. Additive enhancement of neutrophil influx and protein accumulation was observed in the LPS + ultrafine TiO$_2$ group, as compared with the sum of the effects of ultrafine TiO$_2$ and LPS exposure alone. In parallel, the LPS + ultrafine TiO$_2$ group showed additive enhancement of levels of ROS and both mRNA and proteins for proinflammatory mediators. Contrary to this trend, a synergistic effect was noted for TNF-α at the levels of protein and mRNA expression. In agreement, a synergistic effect of ultrafine TiO$_2$ on TNF-α production was also reported in RAW 264.7 cells stimulated with LPS (Kang et al., 2008). Additive activation of c-Src and the NF-κB pathway in lung tissue by exposure to ultrafine TiO$_2$ was also observed in lungs primed by LPS.

In summary, a well-defined mouse model exhibiting acute pulmonary inflammation after ip exposure to ultrafine TiO$_2$ is described. In general, ultrafine TiO$_2$ exposure in LPS-treated mice resulted in additive effects on neutrophil influx, protein accumulation in BAL fluid, ROS generation in BAL cells, and production of proinflammatory mediators, such as IL-1β and
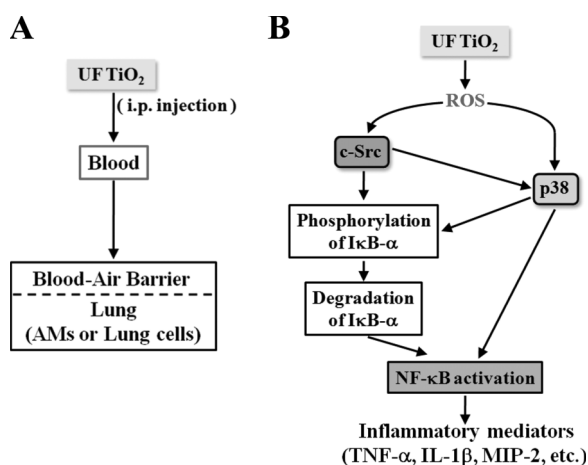
FIGURE 7. Diagram depicting translocation of ultrafine TiO$_2$ passage after ip injection to the lung (A). A scheme illustrating the proposed inflammatory signaling pathways leading to transcription of proinflammatory genes in lung cells or alveolar macrophages after ultrafine TiO$_2$ exposure (B).

MIP-2, but with a synergistic effect seen for TNF-α. Oxidant-dependent inflammatory signaling cascades, including activations of c-Src, p38 MAP kinase, and NF-κB pathway, appear to play an important mechanistic role in inflammatory responses to ultrafine TiO$_2$ exposure. However, the effects observed here were only for the P-25 TiO$_2$ (80% anatase and 20% rutile) tested and cannot be extrapolated to other TiO$_2$ nanoparticles or nanomaterials that may have different physicochemical characteristics (mineral type, crystallinity, size distribution, or surface property/reactivity). A diagram depicting translocation of ultrafine TiO$_2$ to the lung following ip injection and a schematic summary of the proposed inflammatory signaling pathways leading to transcription of proinflammatory genes in lung cells or alveolar macrophages after ultrafine TiO$_2$ exposure are given in Figure 7, A and B, respectively.

REFERENCES

Abu-Amer, Y., Ross, F., McHugh, K., Livolsi, A., Peyron, J. F., and Teitelbaum, S. 1998. Tumor necrosis factor-alpha activation of nuclear transcription factor-kappaB in marrow macrophages is mediated by c-Src tyrosine phosphorylation of Ikappa B alpha. *J. Biol. Chem.* 273:29417–29423.

Ayon, A. A., Cantu, M., Chava, K., Agrawal, C. M., Feldman, M. D., Johnson, D., Patel, D., and Marton, D. 2006. Drug loading of nanoporous TiO$_2$ films. *Biomed. Mater.* 1:L11–L15.

Bermudez, E., Mangum, J. B., Wong, B. A., Asgharian, B., Hext, P. M., Warheit, D. B., and Everitt, J. I. 2004. Pulmonary responses of mice, rats, and hamsters to subchronic inhalation of ultrafine titanium dioxide particles. *Toxicol. Sci.* 77:347–357.

Blackwell, T. S., Blackwell, T. R., Holden, E. P., Christman, B. W., and Christman, J. W. 1996. *In vivo* antioxidant treatment suppresses nuclear factor-kappa B activation and neutrophilic lung inflammation. *J. Immunol.* 157:1630–1637.

Castranova, V., Jones, T., Barger, M. W., Afshari, A., and Frazer, D. J. 1990. Pulmonary responses of guinea pigs to consecutive exposures to cotton dust. In *Proceedings of the 14th Cotton Dust Research Conference*, eds. R. R. Jacobs, P. J. Wakelyn, and L. N. Domelsmith, pp. 131–135. Memphis, TN: National Cotton Council.

Denis, M., Guojian, L., Widmer, M., and Cantin, A. 1994. A mouse model of lung injury induced by microbial products: Implication of tumor necrosis factor. *Am. J. Respir. Cell Mol. Biol.* 10:658–664.

Ding, M., Shi, X., Dong, Z., Chen, F., Lu, Y., Castranova, V., and Vallyathan, V. 1999. Freshly fractured crystalline silica induces activator protein-1 activation through ERKs and p38 MAPK. *J. Biol. Chem.* 274:30611–30616.

Dockery, D. W, and Pope, C. A. 1994. Acute respiratory effects of particulate air pollution. *Annu. Rev. Public Health* 15:107–132.

Drouet, C., Shakhov, A. N., and Jongeneel, C. V. 1991. Enhancers and transcription factors controlling the inducibility of the tumor necrosis factor-α promoter in primary macrophages. *J. Immunol.* 147:1694–1700.

Fabian, E., Landsiedel, R., and Ma-Hock, L. 2008. Tissue distribution and toxicity of intravenously administered titanium dioxide nanoparticles in rats. *Arch. Toxicol.* 82:151–157.

Friedland, J. S., Constantin, D., Shaw, T. C., and Stylianou, E. 2001. Regulation of interleukin-8 gene expression after phagocytosis of zymosan by human monocytic cells. *J. Leukocyte Biol.* 70:447–454.

Hartree, E. F. 1972. Determination of protein: A modification of the Lowry method that gives a linear photometric response. *Anal. Biochem.* 48:422–427.

Huynh, M. L., Malcolm, K. C., Kotaru, C., Tilstra, J. A., Westcott, J. Y., Fadok, V. A., and Wenzel, S. E. 2005. Defective apoptotic cell phagocytosis attenuates prostaglandin E_2 and 15-hydroxyeicosatetraenoic acid in severe asthma alveolar macrophages. *Am. J. Respir. Crit. Care Med.*172:972–979.

Kang, J. L., Jung, H. J., Lee, K., and Kim, H. R. 2006. Src tyrosine kinases mediate crystalline silica-induced NF-κB activation through tyrosine phosphorylation of IκB-α and p65 NF-κB in RAW 264.7 macrophages. *Toxicol. Sci.* 90:470–477.

Kang, J. L., Lee, H. W., Kim, H. J., Lee, H. S., Castranova, V., Lim, C. M., and Koh, Y. 2005. Inhibition of Src tyrosine kinases suppresses activation of nuclear factor-κB, and serine and tyrosine phosphorylation of IκB-α in lipopolysaccharide-stimulated RAW 264.7 macrophages. *J. Toxicol. Environ. Health A* 68:1–20.

Kang, J. L., Moon, C., Lee, H. S., Lee, H. W., Park, E. M., Kim, H. S., and Castranova, V. 2008. Comparison of the biological activity between ultrafine and fine titanium dioxide particles in RAW 264.7 cells associated with oxidative stress. *J. Toxicol. Environ. Health A* 71:478–485.

Khadaroo, R. G., Kapus, A., Powers, K. A., Cybulsky, M. I., Marshall, J. C., and Rotstein, O. D. 2003. Oxidative stress reprograms lipopolysaccharide signaling via Src kinase-dependent pathway in RAW 264.7, macrophage cell line. *J. Biol. Chem.* 278:47834–47841.

Kim, H. J., Lee, H. S., Chong, Y. H., and Kang, J. L. 2006. P38 mitogen-activated protein kinase up-regulates LPS-induced NF-κB activation in the development of lung injury and RAW 264.7 macrophages. *Toxicology* 225:36–47.

Krewski, D., Burnett, R., Jerrett, M., Pope, C.A., Rainham, D., Calle, E., Thurston, G., and Thun, M. 2005. Mortality and long-term exposure to ambient air pollution: Ongoing analyses based on the American Cancer Society cohort. *J. Toxicol. Environ. Health A* 68: 1093–1109.

Kristof, A. S., Goldberg, P., Laubach, V., and Hussain, S. N. 1998. A role of inducible nitric oxide synthase in endotoxin-induced acute lung injury. *Am. J. Respir. Crit. Care Med.* 158:1883–1889.

Lane, F. C., and Mehta, J. R. 1990. *In vitro* human tumor sensitivity assay using cell counting and sizing. *Am. Biotechnol. Lab.* 8:12–27.

Lee, H. S., Moon, C., Lee, H. Y., Park, E. M., Cho, M. S., and Kang, J. L. 2007. Src tyrosine kinases mediate activations of NF-κB and integrin signal during lipopolysaccharide-induced acute lung injury. *J. Immunol.* 179:7001–7011.

López, T., Navarrete, J., Conde, R., Ascencio, J. A., Manjarrez, J., and Gonzalez, R. D. 2006. Molecular vibrational analysis and MAS-NMR spectroscopy study of epilepsy drugs encapsulated in TiO_2-sol-gel reservoirs. *J. Biomed. Mater. Res.* 78A:441–448.

López, T., Recillas, S., Guevara, P., Sotelo, J., Alvarez, M., and Odriozola, J. A. 2008. Pt/TiO2 brain biocompatible nanoparticles: GBM treatment using the C6 model in Wistar rats. *Acta Biomater.* 4:2037–2044.

López, T., Ortiz, E., Quintana, P., and González, R. D. 2007. A nanostructured titania bioceramic implantable device capable of drug delivery to the temporal lobe of the brain. *Colloids Surfaces A* 300:3–10.

Monteiller, C., Tran, L., MacNee, W., Faux, S., Jones, A., Niller, B., and Donalson, K. 2007. The pro-inflammatory effects of low-toxicity low-solubility particles, nanoparticles and fine particles, on epithelial cells *in vitro*: The role of surface area. *Occup. Environ. Med.* 64:609–615.

Muhlfeld, C., Geiser, M., Kapp, N., Gehr, P., and Rothen-Rutishauser, B. 2007. Reevaluation of pulmonary titanium dioxide nanoparticle distribution using the relative deposition index:

Evidence for clearance through microvasculature. *Particle Fibre Toxicol.* 4:7–14.

Nishida, M., Maruyama, Y., Tanaka, R., Kontani, K., Nagaro, T., and Kurose, H. G. 2000. Alpha(i) and G alpha(o) are target proteins of reactive oxygen species. *Nature* 408:492–495.

Oberdörster, G., Oberdörster, E., and Oberdörster, J. 2005. Nanotoxicology: An emerging discipline evolving from studies of ultrafine particles. *Environ. Health Perspect.* 113:823–839.

Olmedo, D. G., Tasat, D. R., Evelson, P., Guglielmotti, M. B., and Cabrini, R. L. 2008a. Biological response of tissue with macrophagic ativity to titanium dioxide. *J. Biomed. Mater. Res.* 84A:1087–1093.

Olmedo, D. G., Tasat, D. R., Guglielmotti, M. B., and Cabrini, R. L. 2008b. Biodistribution of titanium dioxide from biologic compartments. *J. Mater. Sci.* 19:3049–3056.

Pope, C. A., Thun, M. J., Namboodiri, M. M., Dockery, D. W., Evans, J. S., Speizer, F. E., and Heath, C. W. J. 1995a. Particulate air pollution as a predictor of mortality in a prospective study of U.S. adults. *Am. J. Respir. Crit. Care Med.* 151:669–674.

Pope, C. A., Bates, D., and Raizenne, M. 1995b. Health effects of particulate air pollution: Time for reassessment? *Environ. Health Perspect.* 103:472–480.

Renwick, L. C., Brown, D., Clouter, A., and Donaldson, K. 2004. Increased inflammation and altered macrophage chemotactic responses caused two ultrafine particle types. *Occup. Environ. Med.* 61:442–447.

Rhoades, K. L., Golub, S. H., and Economou, J. S. 1992. The regulation of the human tumor necrosis factor-α promoter region in macrophage, T cell, and B cell lines. *J. Biol. Chem.* 267:22102–22107.

Sager, T. M., Kommineni, D., and Castranova, V. 2008. Pulmonary response to intratracheal instillation of ultrafine versus fine titanium dioxide: Role of particle surface area. *Particle Fibre Toxicol.* 5:17–31.

Sager, T. M., Porter, D. W., Robinson, V. A., Lyndsley, W. G., Schwegler-Berry, D. E., and Castranova, V. 2007. Improved method to disperse nanoparticles for *in vitro* and *in vivo* investigation of toxicity. *Nanotoxicology* 1:118–129.

Schwartz, J., 1994. What are people dying of on high pollution days? *Environ. Res.* 64:26–35.

Schwartz, J., Dockery, D. W., and Neas, I. M. 1996. Is daily mortality associated specifically with fine particles? *J. Air Waste Manage. Assoc.* 46:927–939.

Severgnini, M., Takahashi, S., Tu, P., Perides, G., Homer, R. J., Jhung, J. W., Bhavsar, D., Cochran, B. H., and Simon, A. R. 2005. Inhibition of the Src and Jak kinases protects against lipopolysaccharide-induced acute lung injury. *Am. J. Respir. Crit. Care Med.* 171:858–867.

Shaulian, E., and Karin, M. 2002. AP-1 as a regulator of cell life and death. *Nat. Cell Biol.* 4a:E131–E136.

Urban, R., Jacobs, J., Tomlinson, M., Gavrilovic, J., Black, J., and Peoc'h M. 2000. Dissemination of wear particles to the liver, spleen, and abdominal lymph nodes of patients with hip or knee replacement. *J. Bone Joint Surg.* 82-Aa:457–476.

Wang, J., Zhou, G., Chen, C., Yu, H., Wang, T., Ma, Y., Jia, G., Gao, Y., Li, B., Sun, J., Li, Y., Jiao, F., Zhao, Y., and Chai, Z. 2007. Acute toxicity and biodistribution of different sized titanium dioxide particles in mice after oral administration. *Toxicol. Lett.* 168:176–185.

Warheit, D. B., Hoke, R. A., Finlay, C., Maria Donner, E, Reed, K. L., and Sayes, C. M. 2007. Development of a base set of toxicity tests using ultrafine TiO$_2$ particles as a component of nanoparticle risk management. *Toxicol. Lett.*171:99–110.

Warheit, D. B., Webb, T. R., Sayes, C. M., Colvin, V. L., and Reed, K. 2006. Pulmonary instillation studies with nanoparticle TiO$_2$ rods and dots in rats: Toxicity is not dependent upon particle size and surface area. *Toxicol. Sci.* 91:227–236.

Xu, J., Sun, Y., Huang, J., Chen, C., Liu, G., Jiang, Y., Zhao, Y., and Jiang, Z. 2007. Phorokilling cancer cells using highly cell-specific antibody–TiO$_2$ bioconjugates and electroporation. *Bioelectrochemistry* 71:217–222.